Electronic Supplementary Material (ESI) for New Journal of Chemistry.

Ruthenium(II) complex containing cinamic acid derivative inhibits cell cycle progression at G0/G1 and induces apoptosis in melanoma cells

Amanda Alvim Negreti[a], Guilherme Álvaro Ferreira-Silva[a], Carolina Girotto Pressete[a], Rafael Fonseca Miranda[a], Caio C. Candido[b], Angelica E. Graminha[c], Antonio Carlos Doriguetto[b], Ester Siqueira Caixeta[a], João Adolfo Costa Hanemann[d], Angel Maurício Castro Gamero[e], Marilia I. F. Barbosa*[b], Marta Miyazawa*[d], Marisa Ionta*[a]

[a]Institute of Biomedical Sciences, Federal University of Alfenas, zip-code 37130-001, Alfenas, MG, Brazil

[b]Institute of Chemistry, Federal University of Alfenas, zip-code 37130-001, Alfenas, MG, Brazil

[c]Departament of Chemistry, Federal University of São Carlos, zip code 13565-905, São Carlos, SP, Brazil

[d]Department of Clinic and Surgery, School of Dentistry. Federal University of Alfenas, zip-code 37130-001, Alfenas, MG, Brazil

[e]Human Genetics Laboratory, Institute of Natural Science, Federal University of Alfenas, Alfenas, MG, Brazil

*Corresponding author: Marisa Ionta, Marta Miyazawa and Marilia I.F. Barbosa

E-mail adresses: marisa.ionta@unifal-mg.edu.br; marta.miyazawa@unifal-mg.edu.br; mariliaifrazaob@yahoo.com.br

SUMMARY

Figure S14. IR spectrum of (A) L_2 and (B) $[Ru(L_2)(dppb)(bipy)]PF_6$ in KBr.

Figure S15. IR spectrum of (A) L_3 and (B) $[Ru(L_3)(dppb)(bipy)]PF_6$ in KBr.

Figure S16. UV-Vis spectrum of $[Ru(_{L1})(dppb)(bipy)]PF_6$ in CH_2Cl_2.

Figure S17. UV-Vis spectrum of $[Ru(L_2)(dppb)(bipy)]PF_6$ in CH_2Cl_2.

Figure S18. UV-Vis spectrum of $[Ru(L_3)(dppb)(bipy)]PF_6$ in CH_2Cl_2.

Figure S19. cyclic voltammogram of (A) $[Ru(L_1)(dppb)(bipy)]PF_6$. (B) $[Ru(L_2)(dppb)(bipy)]PF_6$, , (C) $[Ru(L_3)(dppb)(bipy)]PF_6$.

Figure S20. Cell viability determined by MTS assay in HT-144 cell line after 24 h of the treatment with ligands L_1, L_2 or L_3.

Figure S21. Cell viability determined by Trypan blue exclusion assay in CHL-1 cell line after 24 h of the treatment with $[Ru(L_2)(dppb)(bipy)]PF_6$ (complex **2**).

Table 1S. chemical shifts and coupling constants of the complexes

Table 2S. IR frequencies

Table 3S. Electrochemical potentials of the complexes

Table 4S. Selectivity indexes using CCD-1059Sk as reference of non-tumor cells.

Table 5S. Selectivity indexes using FB1 as reference of non-tumor cells.

Table 6S. Selectivity indexes using NGM as reference of non-tumor cells.

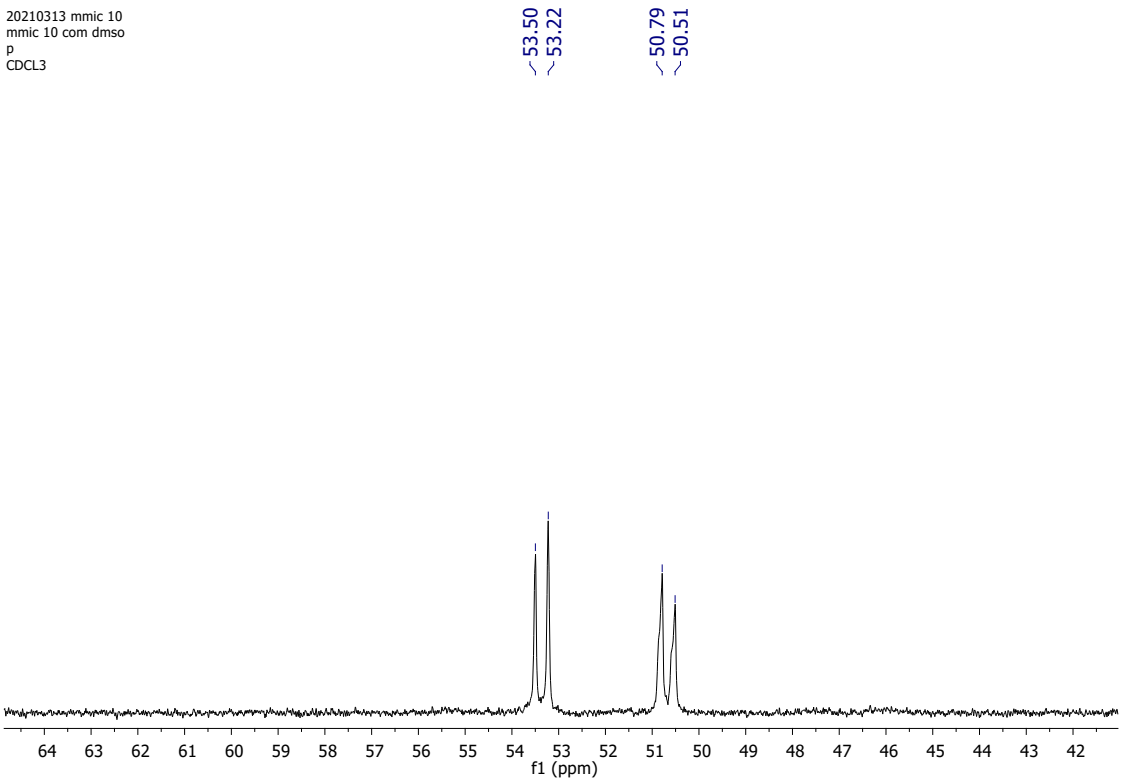

Figure S1: $^{31}P\{^{1}H\}$ spectrum of $[Ru(L_1)(dppb)(bipy)]PF_6$, in CH_2Cl_2.

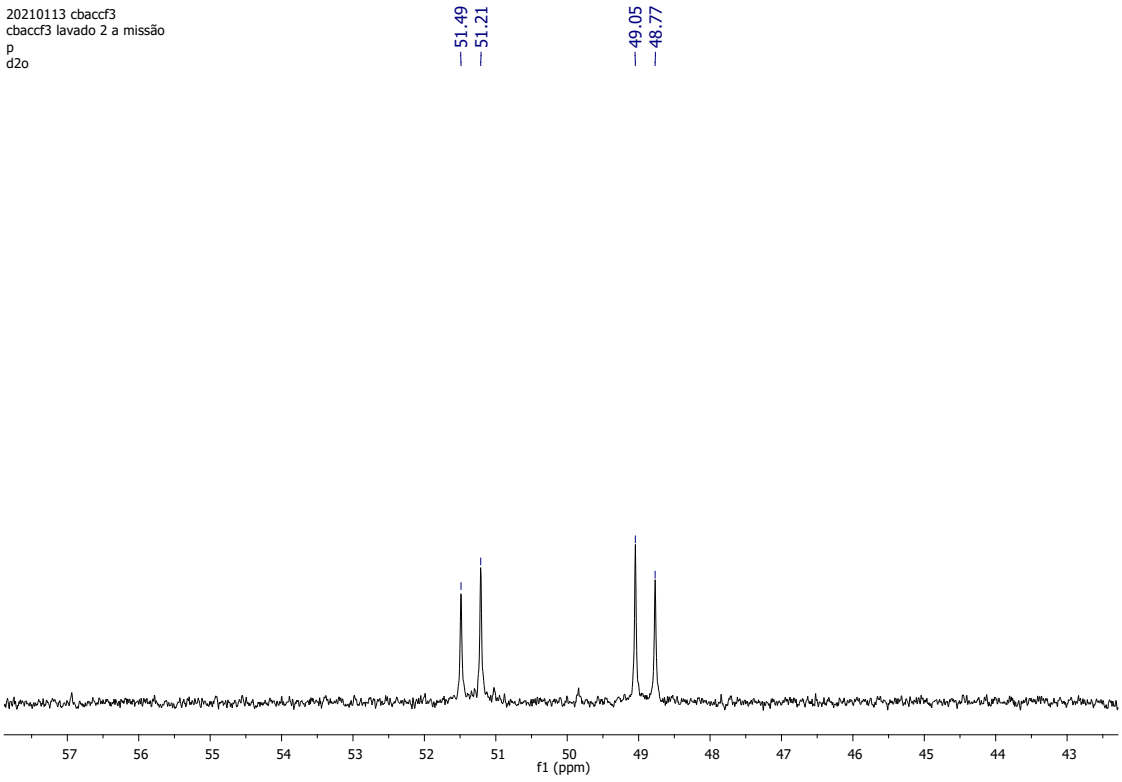

Figure S2: $^{31}P\{^{1}H\}$ spectrum of $[Ru(L_2)(dppb)(bipy)]PF_6$, in CH_2Cl_2.

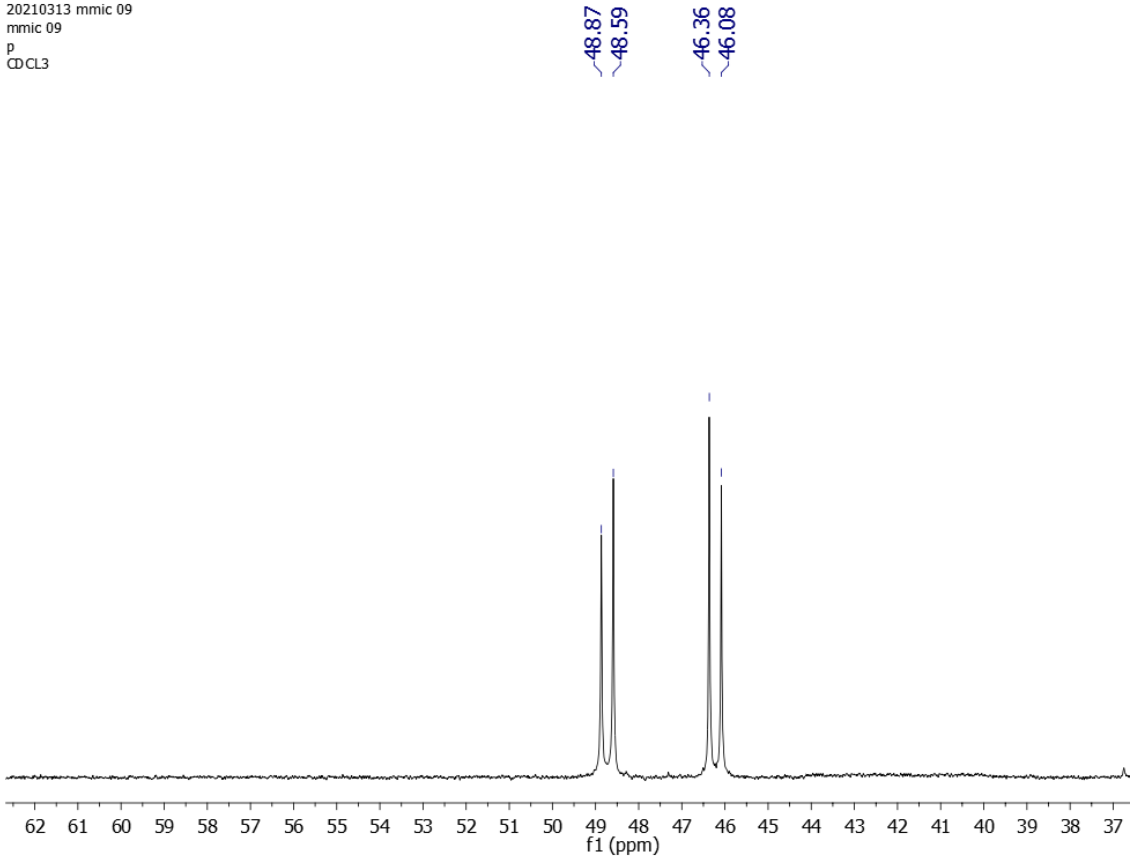

Figure S3: $^{31}P\{^{1}H\}$ spectrum of $[Ru(L_3)(dppb)(bipy)]PF_6$, in CH_2Cl_2.

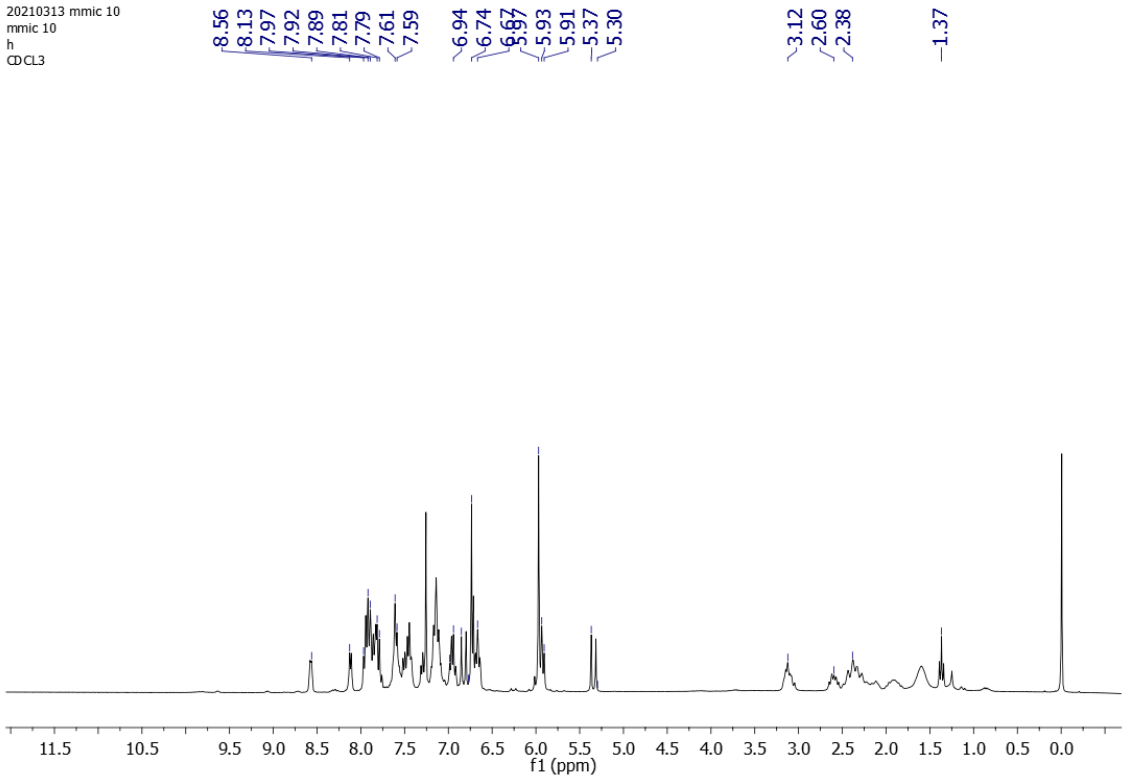

Figure S4: ^{1}H spectrum of [Ru(L_1)(dppb)(bipy)]PF_6, in $CDCl_3$.

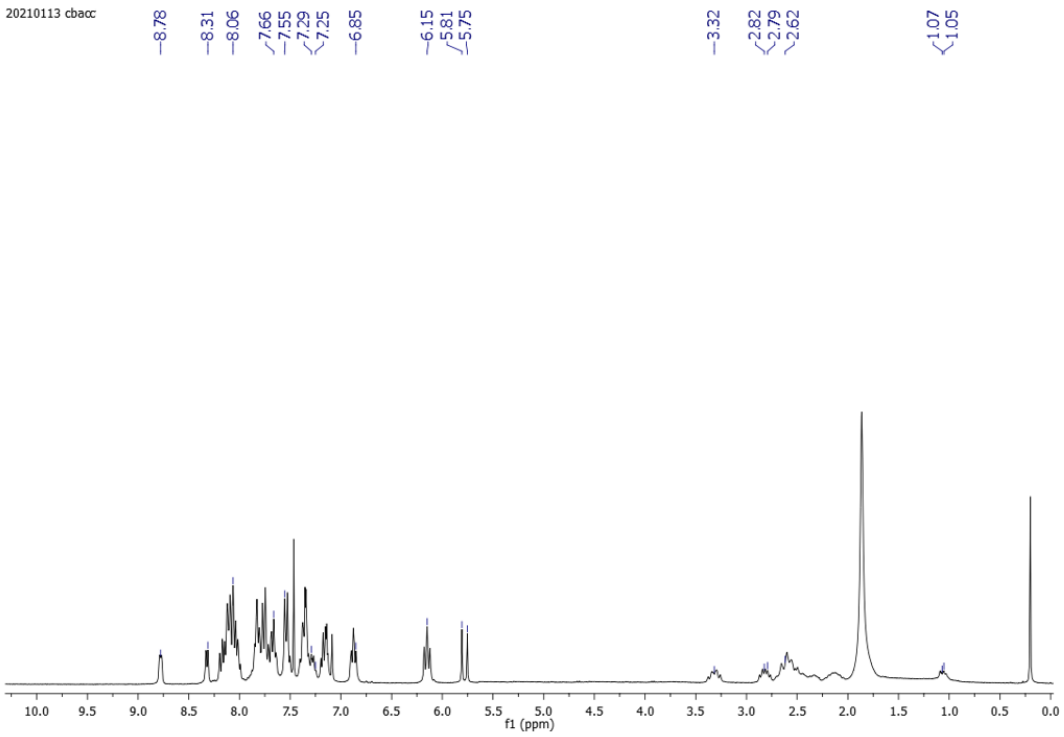

Figure S5: ^{1}H spectrum of [Ru(L_2)(dppb)(bipy)]PF_6, in $CDCl_3$.

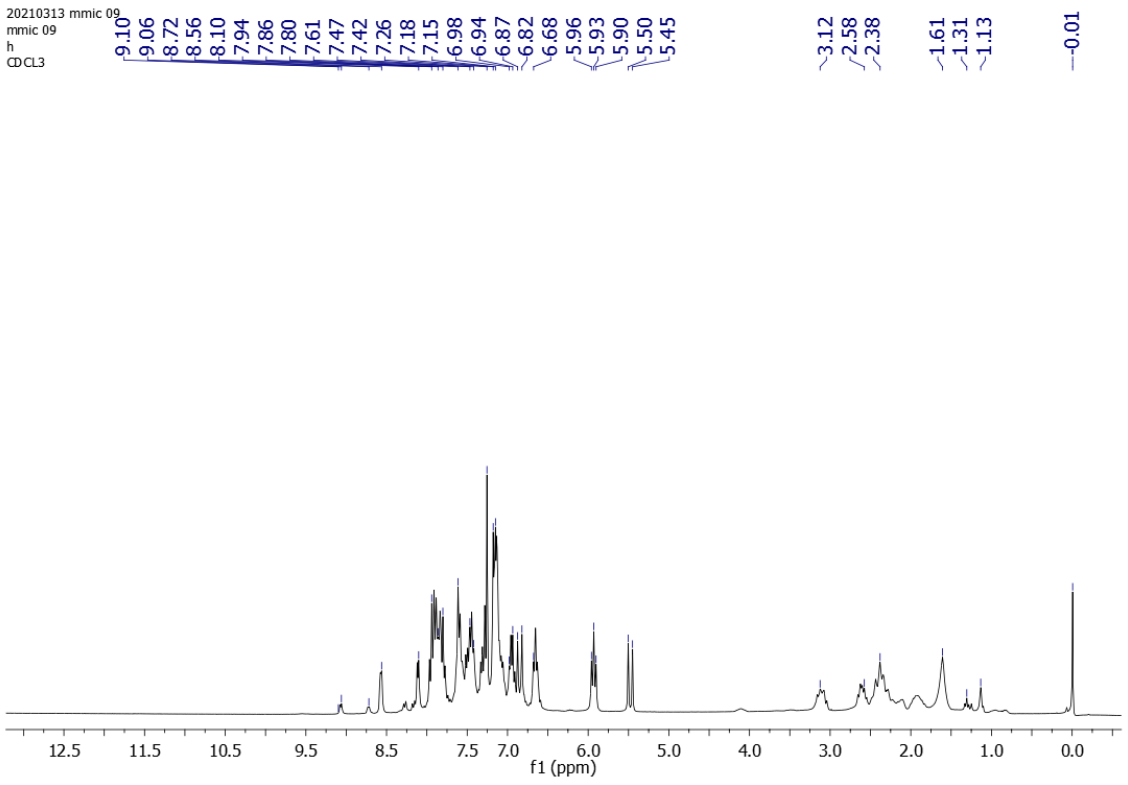

Figure S6: ^{1}H spectrum of [Ru(L_3)(dppb)(bipy)]PF_6, in $CDCl_3$.

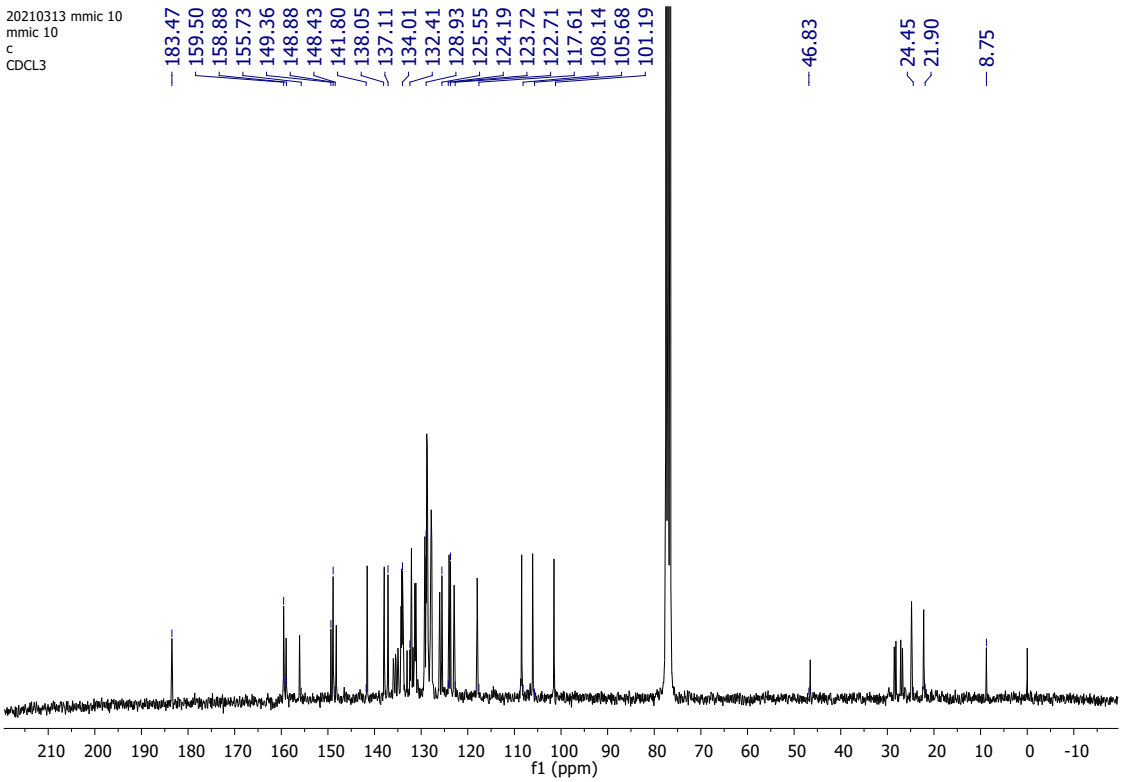

Figure S7: $^{13}C\{^{1}H\}$ spectrum of $[Ru(L_1)(dppb)(bipy)]PF_6$, in $CDCl_3$.

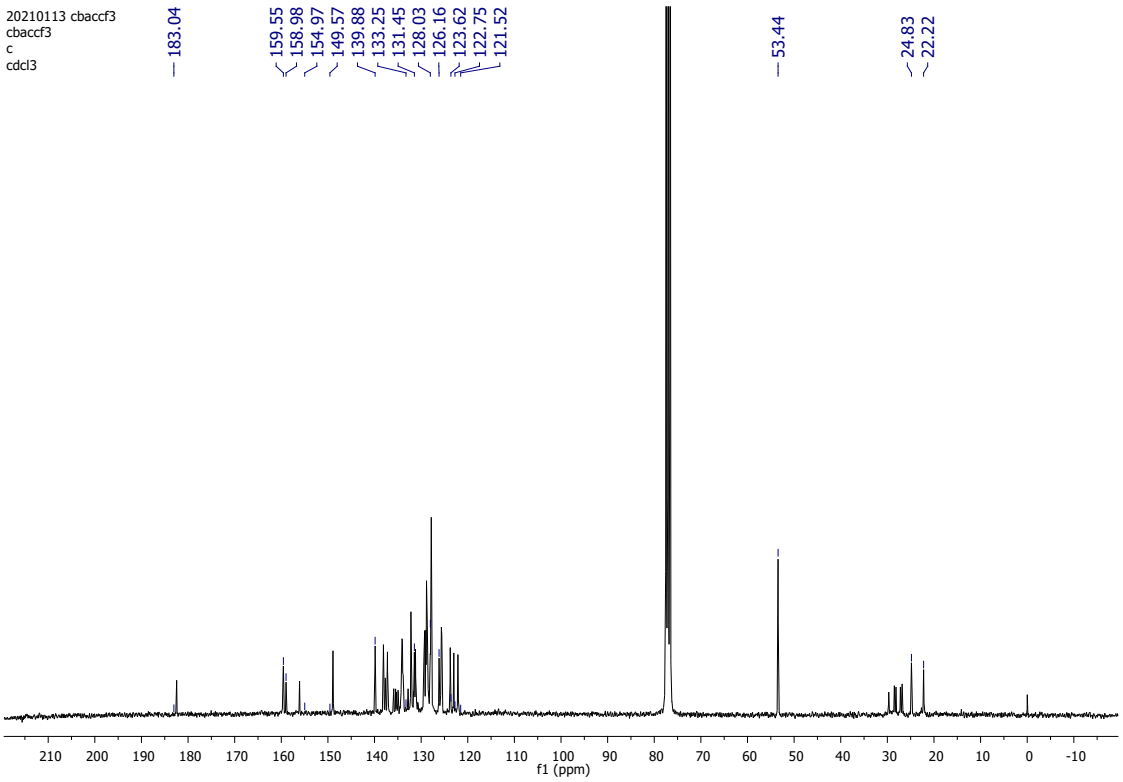

Figure S8: $^{13}C\{^{1}H\}$ spectrum of $[Ru(L_2)(dppb)(bipy)]PF_6$, in $CDCl_3$.

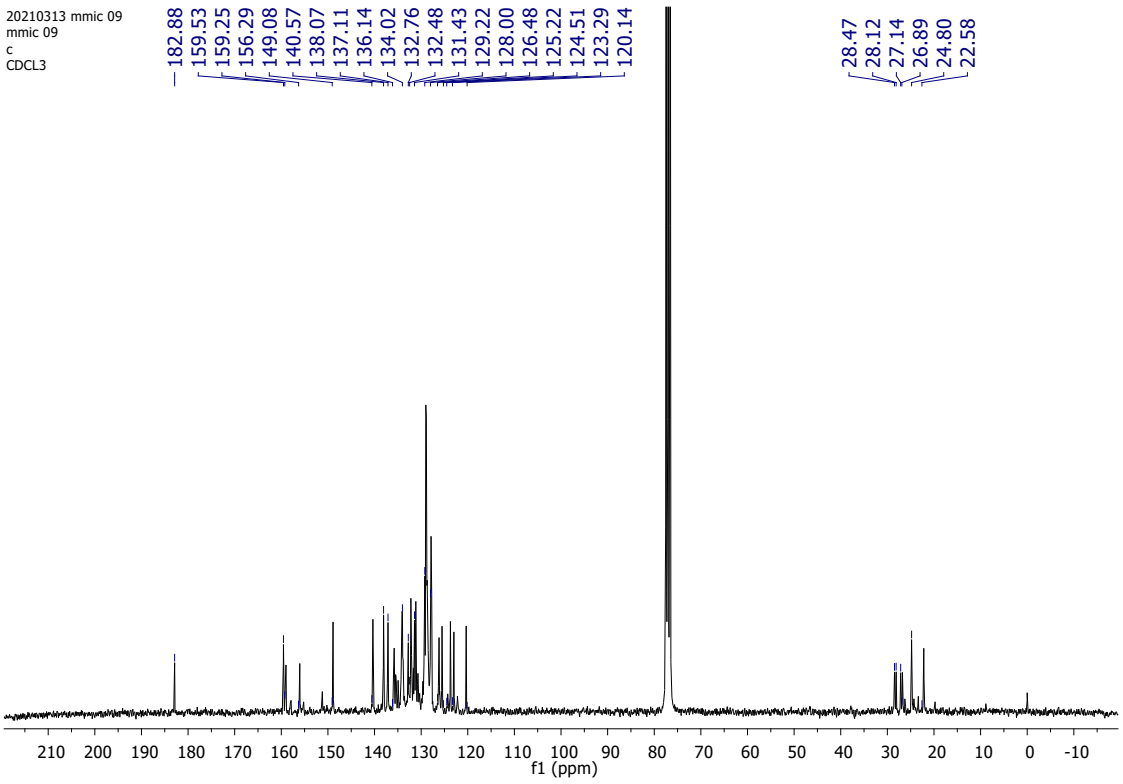

Figure S9: $^{13}C\{^{1}H\}$ spectrum of $[Ru(L_3)(dppb)(bipy)]PF_6$, in $CDCl_3$.

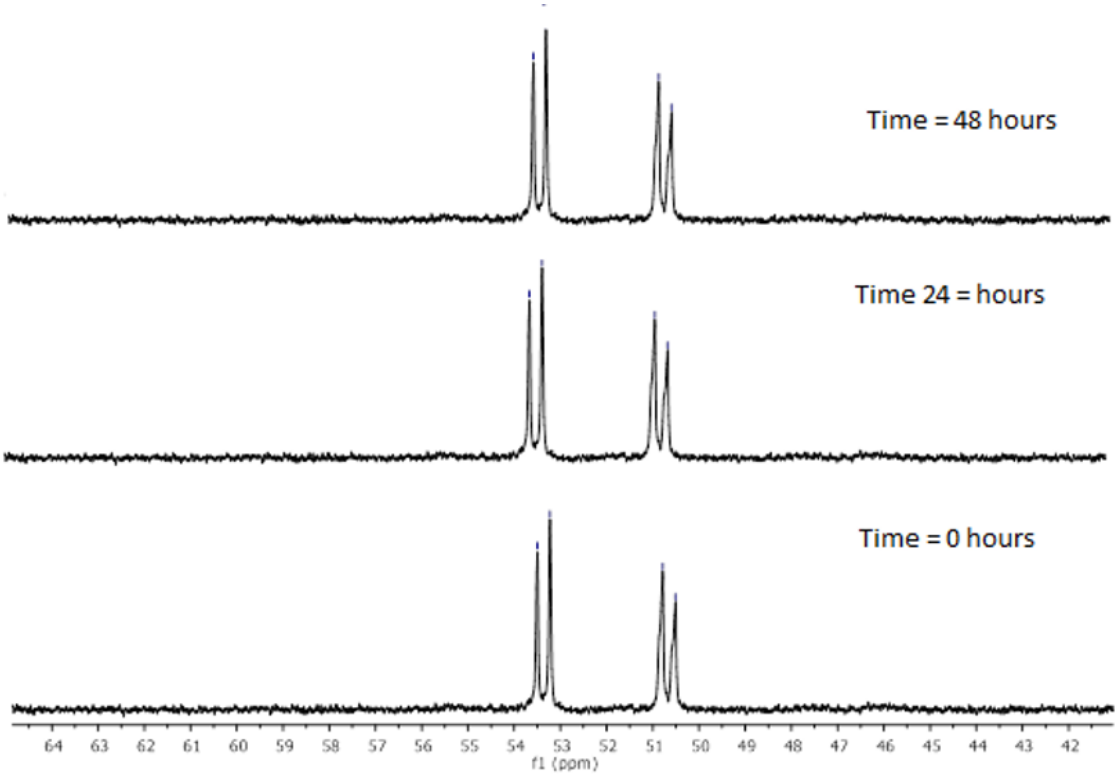

Figure S10: $^{31}P\{^{1}H\}$ NMR spectroscopy of $[Ru(L_1)(dppb)(bipy)]PF_6$: 0 min., 24 h and 48 h, in DMSO-d6

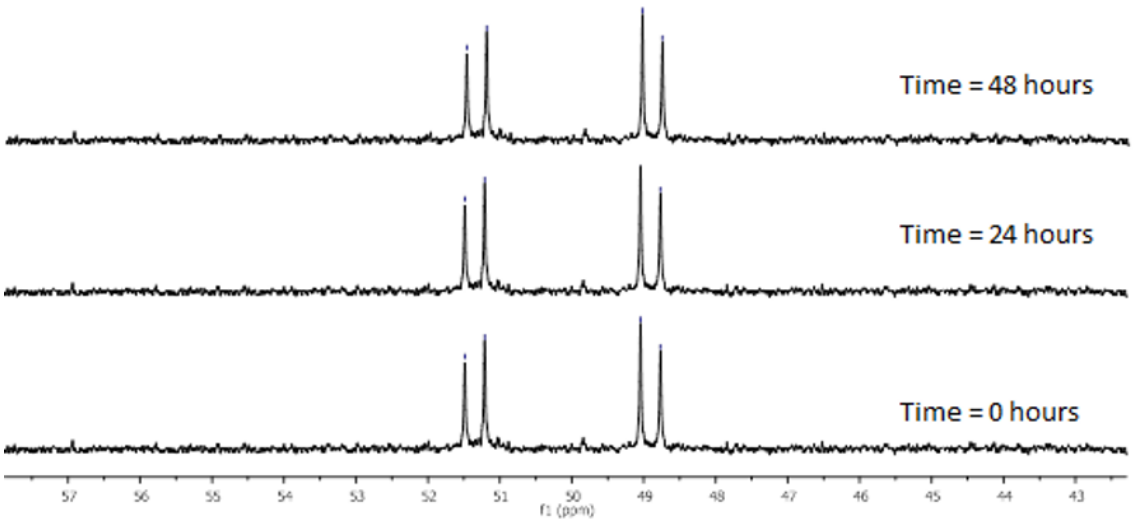

Figure S11: $^{31}P\{^{1}H\}$ NMR spectroscopy of $[Ru(L_2)(dppb)(bipy)]PF_6$: 0 min., 24 h and 48 h, in DMSO-d6

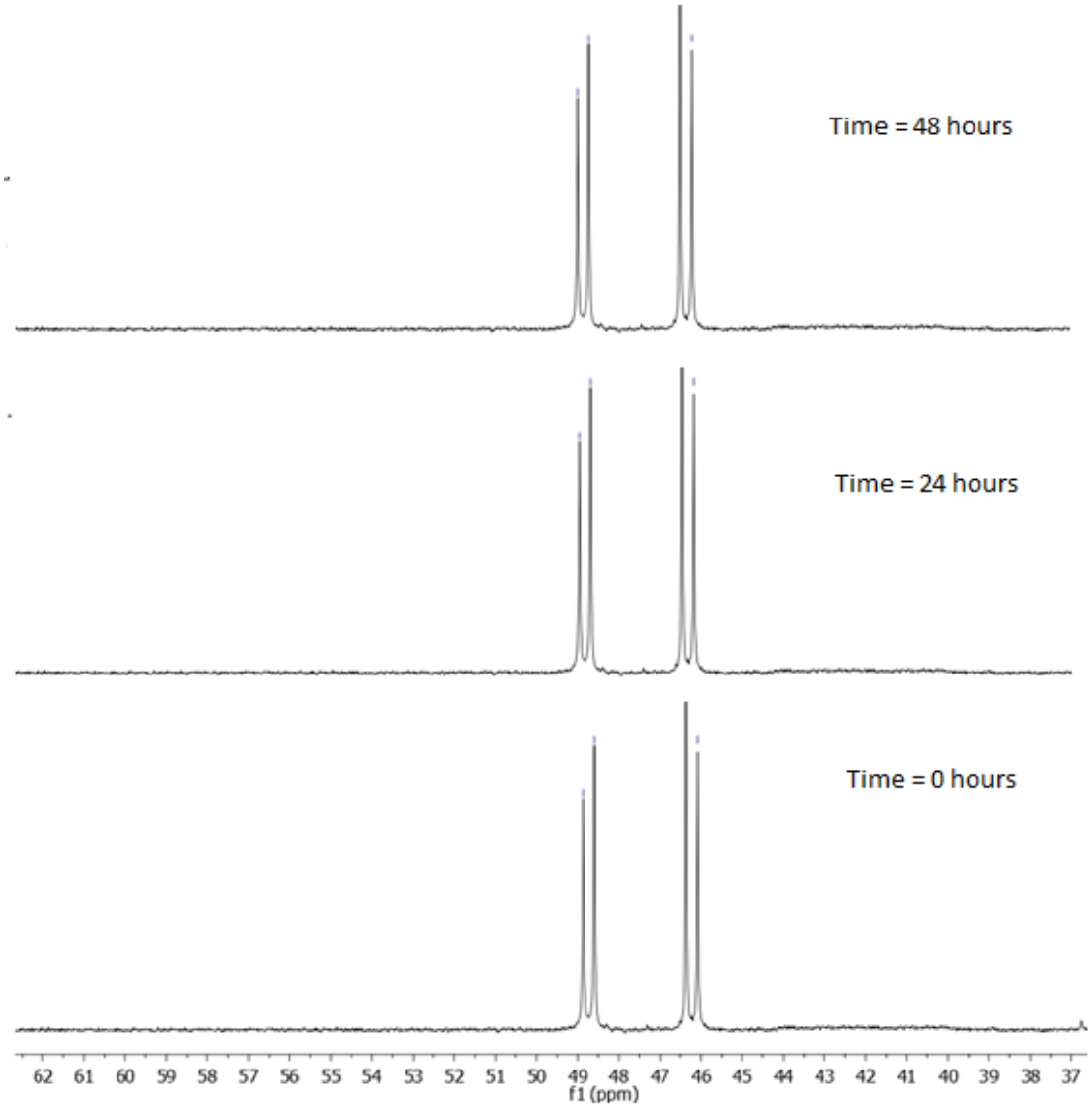

Figure S12: $^{31}P\{^{1}H\}$ NMR spectroscopy of $[Ru(L_3)(dppb)(bipy)]PF_6$: 0 min., 24 h and 48 h, in DMSO-d6

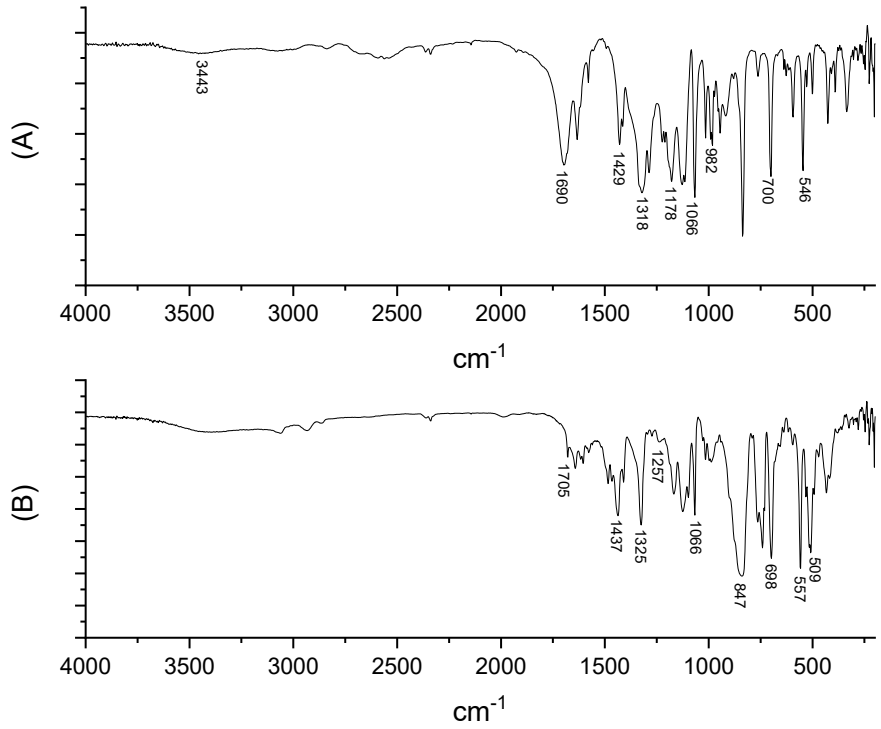

Figure S13: IR spectrum of (A) L1 ligand and (B) [Ru(L1)(dppb)(bipy)]PF_6 in KBr.

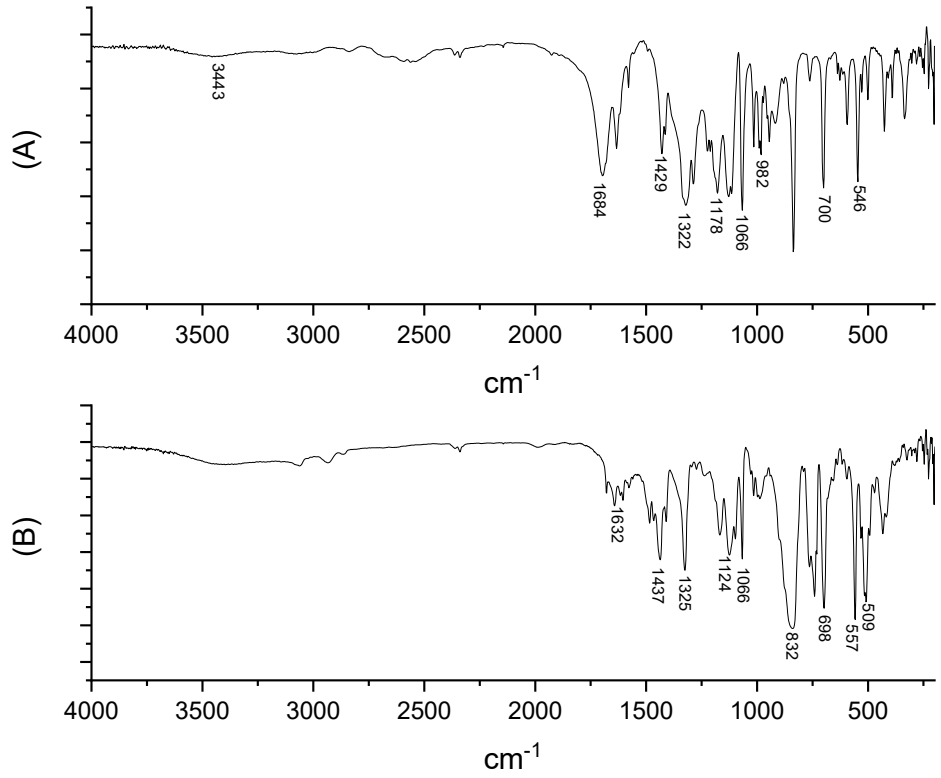

Figure S14: IR spectrum of (A) L2 ligand and (B) [Ru(L2)(dppb)(bipy)]PF_6 in KBr.

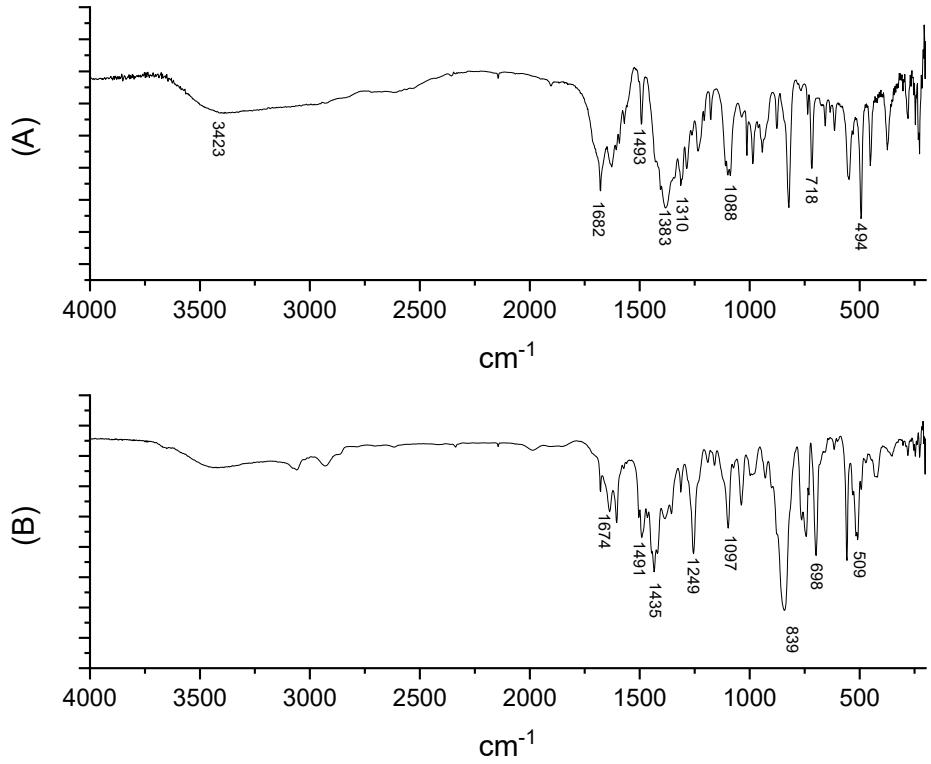

Figure S15: IR spectrum of (A) L3 ligand and (B) [Ru(L3)(dppb)(bipy)]PF6 in KBr.

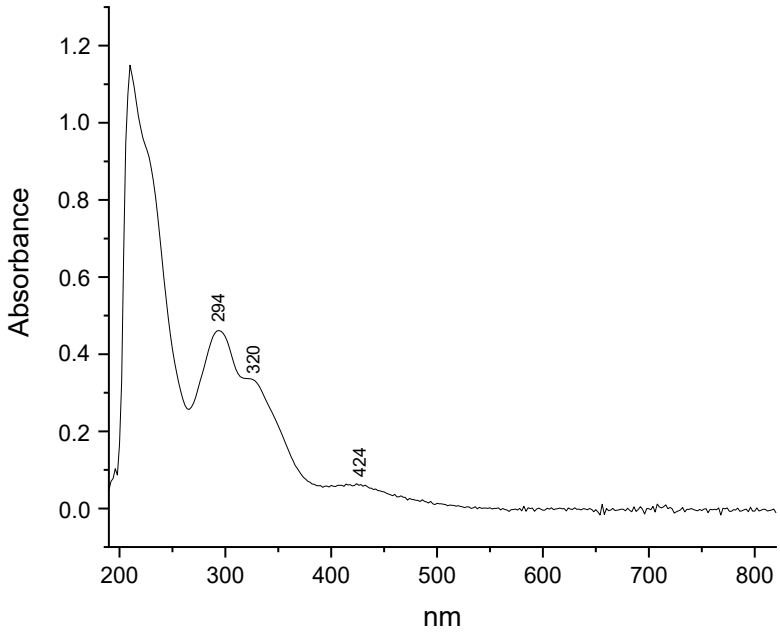

Figure S16: UV-Vis spectrum of [Ru(L1)(dppb)(bipy)]PF_6 in CH_2Cl_2.

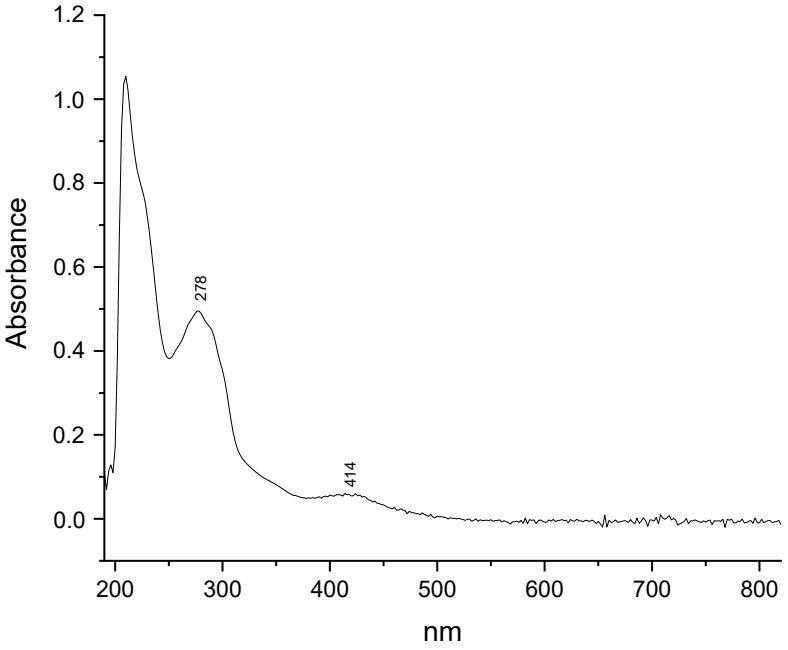

Figure S17: UV-Vis spectrum of [Ru(L2)(dppb)(bipy)]PF_6 in CH_2Cl_2.

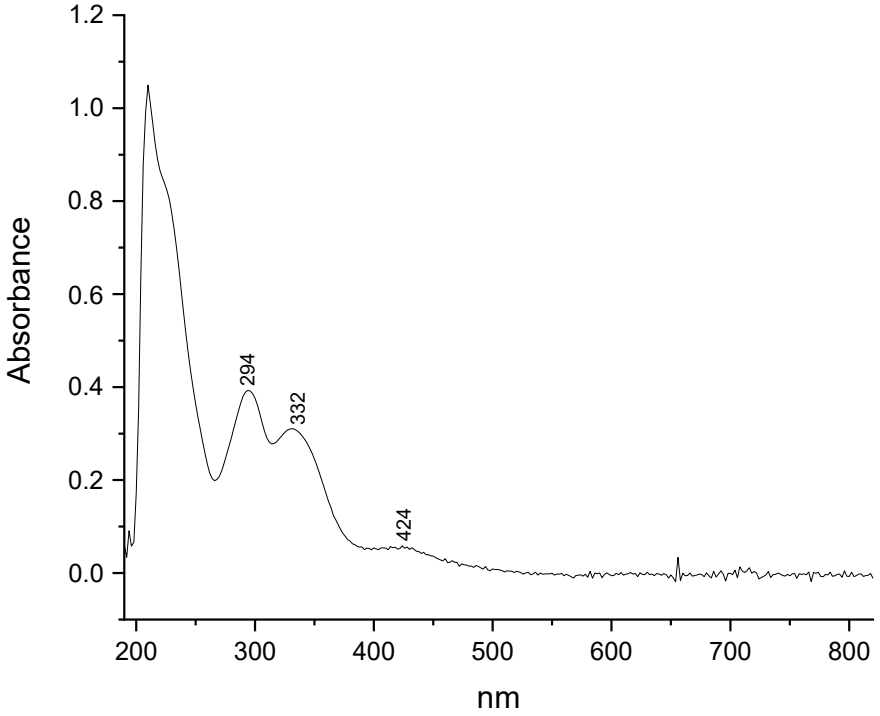

Figure S18: UV-Vis spectrum of [Ru(L3)(dppb)(bipy)]PF_6 in CH_2Cl_2.

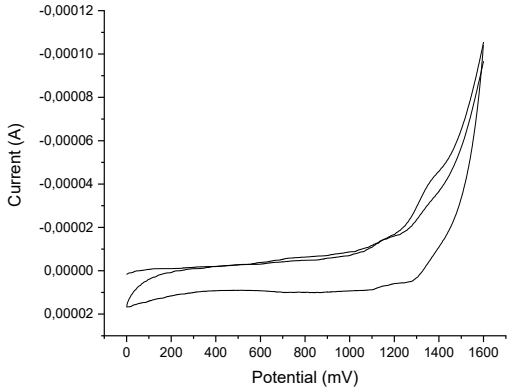

(B)

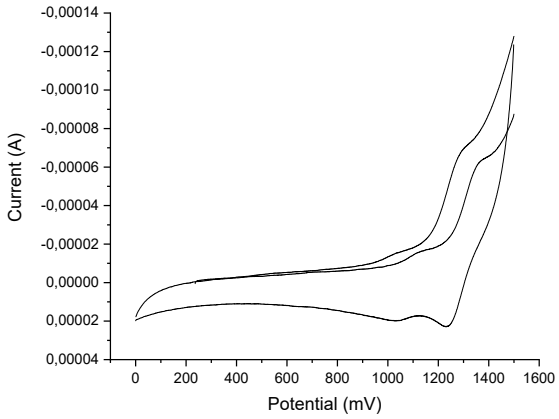

(A)

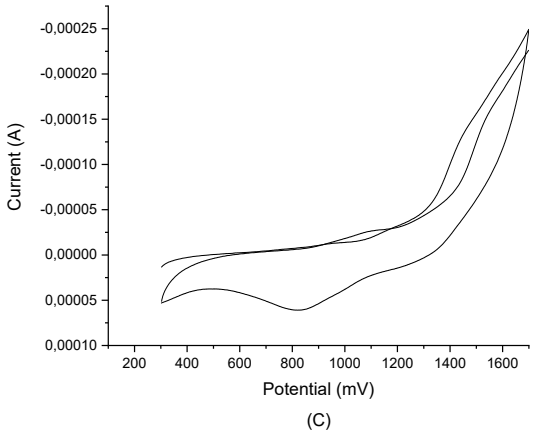

(C)

Figure S19: cyclic voltammogram of (A) [Ru(L1)(dppb)(bipy)]PF_6, (B) [Ru(L2)(dppb)(bipy)]PF_6, (C) [Ru(L3)(dppb)(bipy)]PF_6

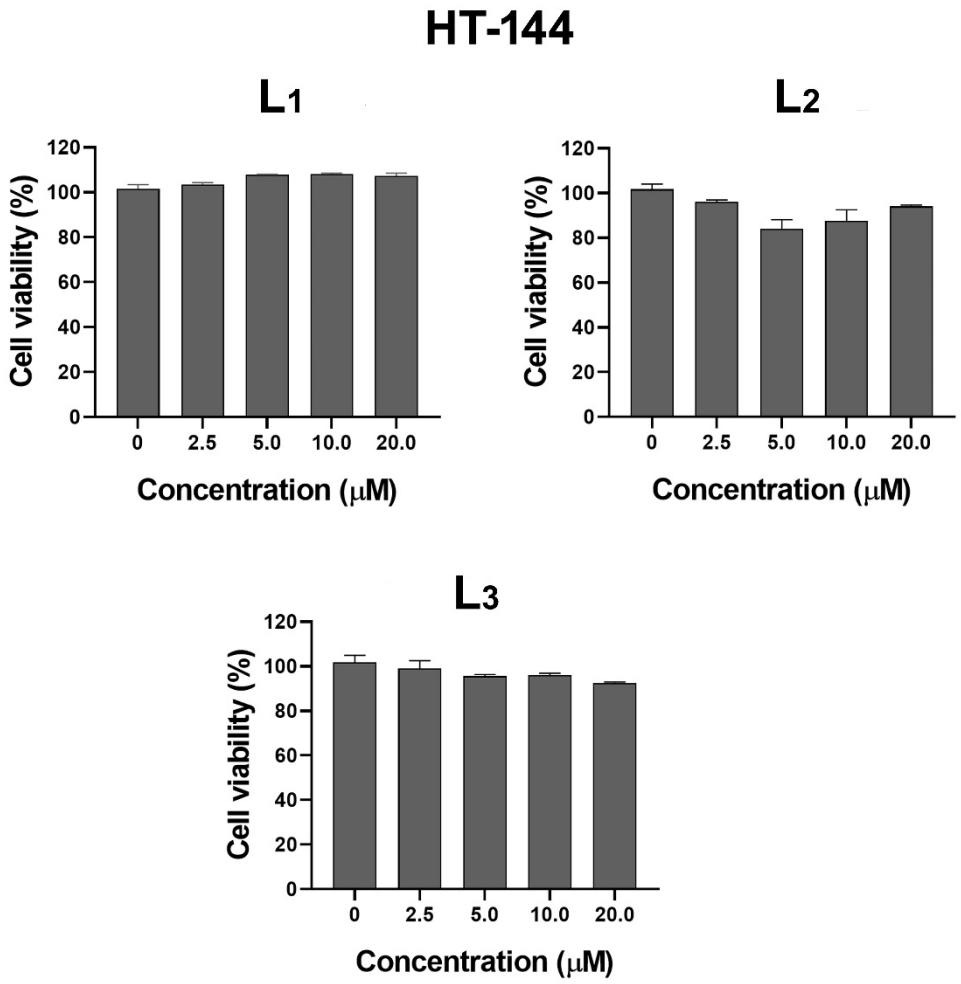

Figure S20. Cell viability determined by MTS assay in HT-144 cell line after 24 h of the treatment with ligands L_1, L_2 or L_3.

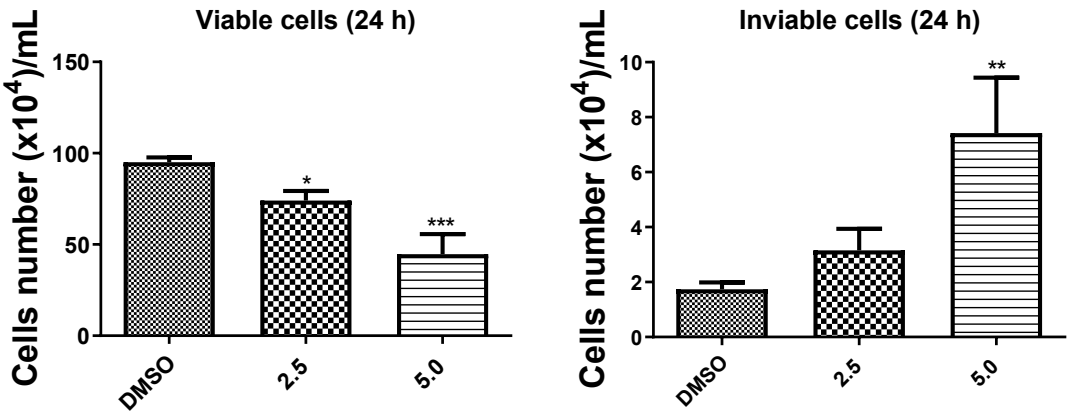

Figure S21. Cell viability determined by Trypan blue exclusion assay in CHL-1 cell line after 24 h of the treatment with complex (**2**). *p<0.05, **p<0.01, ***p<0.001 compared to control group (DMSO).

Table 1S. chemical shifts and coupling constants of the complexes

Compound	δ $^{31}P\{^{1}H\}$ (ppm)	$^{2}Jp\text{-}p$ (Hz)
$[RuCl_2(dppb)(bipy)]$	41.5 / 32.8	30.0
$[Ru(L_1)(dppb)(bipy)]PF_6$	53.4 / 50.6	38.2
$[Ru(L_2)(dppb)(bipy)]PF_6$	45.5 / 46.0	36.8
$[Ru(L_3)(dppb)(bipy)]PF_6$	48.7 / 46.2	38.2

Table 2S. IR carboxylate and counter ion stretching frequencies

Compound	vas(COO^-)	vs(COO^-)	Δv (vas(COO^-) - vs(COO^-))	vsP-F
$[RuCl_2(dppb)(bipy)]$	-	-	-	-
$[Ru(L_1)(dppb)(bipy)]PF6$	1705	1257	448	847
L_1	1690	1318	372	-
$[Ru(L_2)(dppb)(bipy)]PF6$	1632	1290	342	832
L_2	1684	1322	362	-
$[Ru(L_3)(dppb)(bipy)]PF6$	1674	1249	425	839
L_3	1682	1310	372	-

Table 3S. Electrochemical potentials of the complexes

Compound	Ru(II)/Ru(III) (V)	Ru(III)/Ru(II) (V)	E1/2 (V)
$[RuCl_2(dppb)(bipy)]$	0.62	0.57	0.6
$[Ru(L_1)(dppb)(bipy)]PF_6$	1.45	1.40	1.4
$[Ru(L_2)(dppb)(bipy)]PF_6$	1.35	1.29	1.3
$[Ru(L_3)(dppb)(bipy)]PF_6$	1.34	1.28	1.3

Table 4S. Selectivity indexes (SIs) determined using CCD-1059Sk (fibroblast derived from human normal skin) as reference of non-tumor cell line.

Cell line	CINAM	TRANSCINAM	CLOROCINAM
HT-144	2.46	2.97	1.79
SK-MEL-147	1.64	1.50	0.76
CHL-1	**4.63**	**3.30**	2.37
WM1366	0.91	1.34	1.22

Table 5S. Selectivity indexes (SIs) determined using FB1 (fibroblast derived from primary culture established from gingival tissue) as reference of non-tumor cell line.

Cell line	CINAM	TRANSCINAM	CLOROCINAM
HT-144	1.40	**4.26**	1.42
SK-MEL-147	0.94	2.14	0.60
CHL-1	2.64	**4.70**	1.88
WM1366	0.52	1.91	0.97

Table 6S. Selectivity indexes (SIs) determined using NGM as reference of non-tumor cell line.

Cell line	CINAM	TRANSCINAM
HT-144	2.82	2.32
SK-MEL-147	1.88	1.16
CHL-1	**5.31**	**2.5**
WM1366	1.04	1.04